Original paper

Metahewettite, $Ca(V^{5+}_6O_{16})(H_2O)_3$, from Hodzha–Rushnai–Mazar, southern Kirgizia: occurrence and crystal structure

Mark A. COOPER[1], Frank C. HAWTHORNE[1,*], Vladimir Y. KARPENKO[2], Leonid A. PAUTOV[2], Atali A. AGAKHANOV[2]

[1] *Department of Geological Sciences, University of Manitoba, Winnipeg, MB, R3T 2N2, Canada; Frank.Hawthorne@umanitoba.ca*
[2] *Fersman Mineralogical Museum, Russian Academy of Sciences, Moscow, 117071, Russia*
**Corresponding author*

Metahewettite was encountered in hypergene crusts in Paleozoic carbon–silica schists included in the carbon mélange matrix at Hodzha–Rushnai–Mazar in southern Kirgizia. Schist outcrops are marked by multicolored yellow, orange, brown and green crusts of vanadates and sulfates of chalcoalumite group, volborthite, V-bearing phosphates, Cr–V-bearing members of alunite subgroup, members of the pascoite group and vanadium-bronze oxides, including metahewettite. Metahewettite is acicular with individual crystals up to 1 mm in length, and forms radial aggregates 2–3 mm in diameter, or flattened aggregates in narrow fissures. Crystals are dark-brown to reddish-brown with a golden sheen. The crystal structure of metahewettite, $Ca(V^{5+}_6O_{16})(H_2O)_3$, monoclinic, a = 12.208(5), b = 3.6011(15), c = 18.358(7) Å, β = 118.538(8)°, V = 709.0(8) Å^3, Z = 2, $A2/m$, was refined to an R_1 index of 2.4 % based on 1047 unique observed ($F_o > 4\sigma F$) reflections. Electron-microprobe analysis (EDS) showed no detectable constituents apart from Ca and V, and the scattering from each site in the structure is conformable with the ideal composition $Ca(V_6O_{16})(H_2O)_3$. There are three *V* sites in the structure with scattering in accord with their complete occupancy by V. The *V*(1) site is [5]-coordinated by O^{2-} anions with a <*V*–O> distance of 1.823 Å and a [2 + 3] arrangement of vanadyl <1.67 Å> and equatorial (<1.925 Å>) bonds. The *V*(2) and *V*(3) sites are coordinated by O^{2-} anions with <*V*–O> distances of 1.934 and 1.916 Å and [2 + 2 + 2] and [1 + 4 + 1] arrangements of vanadyl <1.652 Å>, equatorial <1.906 Å> and *trans* <2.237 Å> bonds, respectively. The *V*(1) square pyramids share edges and vertices to form chains extending parallel to **b** with a repeat distance of 3.6 Å. The *V*(2) and *V*(3) octahedra share edges and vertices to form ribbons also extending parallel to **b**. The chains and ribbons link by sharing polyhedron corners to form sheets of V polyhedra parallel to (001). These sheets are linked by interlayer Ca that occupies two interstitial *Ca* sites, and by (H_2O) groups.

Keywords: metahewettite, crystal structure, vanadium-bronze oxide, occurrence, Kirgizia
Received: 11 December 2013; accepted: 1 April 2014; handling editor: J. Plášil
The online version of this article (doi: 10.3190/jgeosci.167) contains supplementary electronic material.

1. Introduction

Evans and Hughes (1990) divided the known vanadium-bronze minerals into three groups: (1) the hewettite group, (2) the straczekite group, and (3) other structure types. The hewettite group includes hewettite and metahewettite (Hillebrand et al. 1914; Bachmann and Barnes 1962), barnesite (Weeks et al. 1963; Ankinovich and Podlepaeva 1986), hendersonite (Lindberg et al. 1962) and grantsite (Weeks et al. 1964), all of which have structures similar to that of $Li_3V_6O_{16}$ (Wadsley 1957; Evans 1989). These structures, some of the fibrous vanadium-bronzes (fiber spacing 3.6 Å), consist of lateral linkages (into sheets or frameworks) of two types of vanadate chains: (1) a $[V_2O_6]_n$ chain consisting of alternating square pyramids, and (2) a $[V_4O_{12}]_n$ chain consisting of four highly condensed single chains of octahedra. Experimentally, these minerals are rather difficult to deal with as they show reversible hydration–dehydration with accompanying order–disorder giving poorly resolved diffraction patterns and hence poorly resolved structures. In addition, helical distortion of the fibrous crystals around their length is common, further decreasing resolution in the diffraction patterns. There may be Ca–Na disorder (Barnes 1955) and Ca–Sr substitution (Evans and Hughes 1990), further reducing the diffraction quality of the crystals.

Hewettite and metahewettite are conventionally written as $Ca(V^{5+}_6O_{16})(H_2O)_9$ and $Ca(V^{5+}_6O_{16})(H_2O)_3$, respectively, although Qurashi (1961) reported an intermediate phase $Ca(V^{5+}_6O_{16})(H_2O)_6$. The cell dimensions are as follows: hewettite: a = 12.27, b = 3.60, c = 11.17 Å, β = 97.2° (averaged from the data of Bayliss 1982 and Evans 1989), and metahewettite: a = 12.15, b = 3.61, c = 9.22 × 2 Å, β = 118.2° (Evans 1989). Thus the cell dimensions of each mineral are fairly distinct, but detailed work by Hillebrand et al. (1914) and Qurashi (1961) has shown that these minerals are very sensitive to the ambient humidity.

2. Occurrence

Metahewettite was encountered in hypergene crusts in Paleozoic carbon–silica schists included in the carbon mélange matrix at Hodzha–Rushnai–Mazar in southern Kirgizia (Batken region, Isfairam River basin). It is part of a chain of olistolite blocks along the south part of the Fergana Valley with high trace-element contents of U, V, Mo, Ni, Zn and Cu. This location was initially explored by the Radium Expedition of 1911–1918 headed by V. I. Vernadsky in connection with surveying the famous Tuya–Muyun U–V–Ra deposit. Later work was done by the Commission on Investigation of Natural Productive Forces of Russia (KEPS) (Scherbakov 1924; Fersman 1928). Some of the olistolite blocks (Kara–Chagyr, Okhna) were prospected for U in 1940–1950, and the largest (Kara–Tangi) was mined for U in the 1970s.

Schist outcrops are marked by multicolored yellow, orange, brown and green crusts, which were called "kolovratites" by early geologists as they often contained Ni and V, which are the main components of kolovratite, a mineral first described from Kara–Chagyr (Vernadsky 1922). Recent work (Karpenko 2010) showed that the compositions of these crusts are very complicated. They consist of vanadates and sulfates of the chalcoalumite group (Hawthorne and Cooper 2013): alvanite (Pertlik and Dunn 1990), ankinovichite (Karpenko et al. 2004a), nickelalumite (Karpenko et al. 2004b; Uvarova et al. 2005), kyrgyzstanite (Agakhanov et al. 2005), volborthite, V-bearing phosphates, Cr–V-bearing members of the alunite subgroup, members of the pascoite family, and vanadium-bronze oxides including metahewettite. Metahewettite was collected from the old exploration trench at Hodzha–Rushnai–Mazar, 2 km east of the village of Valakish (40º10'15"N 72º 06'33"E).

Fig. 2 Crystals of metahewettite with V-bearing alunite–jarosite (yellow, orange). Field of view: 5 × 7 mm. Photo by N. A. Pekova.

Metahewettite is acicular with individual crystals up to 1 mm in length (Fig. 1), and forms radial aggregates 2–3 mm in diameter, or flattened ones (Fig. 2) in narrow fissures. Crystals are dark-brown to reddish-brown with a golden sheen. Crystals used for structural investigation show no visible inclusions or heterogeneity. Metahewettite is associated with vanadium-bearing phosphates (V_2O_3 from 0 to 5 wt. %): nevadaite (Fig. 3), leucophosphite, kingite, minyulite, fluellite and variscite, plus aggregates of alunite–jarosite (V_2O_3 up to 4.5 wt. %, Cr_2O_3 up to 4.0 wt. %), pascoite-group minerals (hummerite, magnesiopascoite(?) and an unknown K–Ca–V

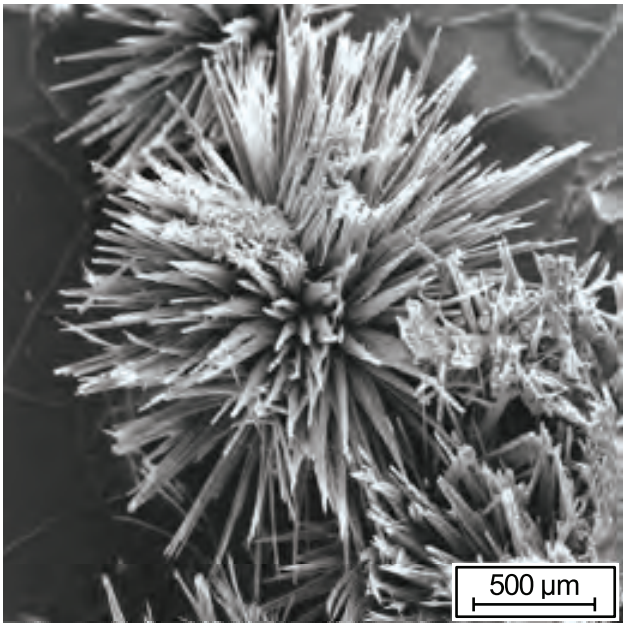

Fig. 1 Metahewettite spherulite (1 mm diameter). SEM photo by L. A. Pautov and V. Y. Karpenko.

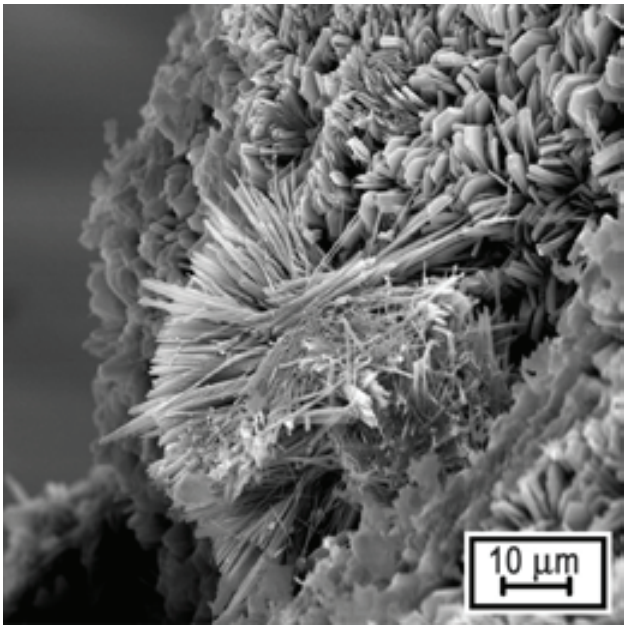

Fig. 3 Acicular crystals of metahewettite on nevadaite. SEM photo by L. A. Pautov and V. Y. Karpenko.

mineral), gypsum, calcite, opal and hemimorphite (Karpenko et al. 2009; Karpenko 2010).

3. Experimental

The sample of metahewettite examined here is a radiating mass of deep reddish-brown flattened fibers, with individual fibers often displaying helical twists. The unit cell for metahewettite was first reported as monoclinic *A*-centered with a = 12.25, b = 3.615, c = 2 × 9.27 Å, β = 118°, from Weissenberg film data on a poor-quality single-crystal with streaked reflections (Qurashi 1961). The unit cell was later refined from X-ray powder-diffraction data conformable with the space group *A*2/*m*, and giving a = 12.15(1), b = 3.607(3), c = 18.44(1) Å, β = 118.03(5)° (Bayliss and Warne 1979). As noted above, these values are quite distinct from those of hewettite and initially served to identify our sample as metahewettite.

3.1. X-ray data collection

An ultra-thin fiber ~2 μm thick was used for collection of X-ray intensity data. It was highly uniform in color, transparency and extinction, with a barely detectable fiber twist (variable over its length). It was attached to a tapered glass fiber and mounted on a Bruker D8 three-circle diffractometer equipped with a rotating-anode generator (MoK_α X-radiation), multilayer optics and an APEX-II detector. Although some minor elongation was present within the spot profiles (presumably due to the extreme variation in physical dimensions of the crystal), the general diffraction pattern was of remarkably high quality (i.e., no streaking, no splitting, no satellites or additional diffraction spots, only crisp spots with sharp boundaries belonging to a single metahewettite crystal domain). This diffraction behavior is very atypical of natural vanadium-bronze structures (e.g., Evans 1989); even synthetic substituted analogues of hewettite show elongated diffraction spots (Oka et al. 1998). We note that on our diffractometer, the X-ray beam-diameter is approximately 120 μm, and that only about ¼ of the crystal length was exposed to the X-ray beam during collection of the X-ray intensity data. The crystal was positioned in the X-ray beam such that the helical twist of the fiber in the beam path was at a minimum; this was done by carefully observing the reflectance details of a bright light reflecting off the crystal surface upon crystal rotation, and resulted in a superior-quality diffraction pattern. In excess of a Ewald sphere of diffraction data was collected (12219 intensities) to 60° 2θ using 30 s frames, a 0.3° frame width and a crystal-to-detector distance of 5 cm. Empirical absorption corrections (SADABS; Sheldrick 2008) were applied and equivalent reflections were averaged, resulting in 4091 individual reflections within the Ewald sphere, and 1182 unique reflections in the Laue group 2/*m*. A large number of intensities (12,219) were collected, several times the number of reflections in the Ewald sphere (4091, Tab. 1). This high degree of overdetermination allows accurate correction for absorption, crystal shape and the variable amount of the crystal in the X-ray beam with crystal orientation. The general observance of higher angle data was reasonable from such a small diffracting volume (i.e., the mean $I/\sigma I$ for all reflections out to 55° 2θ was in excess of 20), and the observance of this higher angle data helped to provide greater spatial detail in our refined structure model.

3.2. Structure solution and refinement

The structure was solved by direct methods in the space group *A*2/*m*, with all atoms initially refining on a mirror plane at y = (0, ½). Conversion to an anisotropic-displacement model in the later stages of refinement showed large atom displacements at the *Ca*(1) and OW(2) sites. The *Ca*(1) site was allowed to refine off its initial 2*d* position (½, 0, 0 with site symmetry 2/*m*) and converged just off the 2-fold axis (but still on the mirror) at the 4*i* position (0.5139, 0, 0.0073). The *Ca*(1) site lies 0.32(3) Å from its symmetrically equivalent counterpart *Ca*(1)′ on the other side of the 2-fold axis, and hence only one of two locally associated *Ca*(1) and Ca(1)′ sites can be occupied. The refined site-occupancy for the *Ca*(1) site is 0.25; thus half of the locally associated Ca(1)–Ca(1)′ pairs are occupied by Ca and □ (or □ and Ca) and half by □ and □. The *Ca*(2) site refined to a 4*i* position (0.1056, ½, 0.03623), significantly displaced from the 2*b* position (0, ½, 0 with site symmetry 2/*m*). The *Ca*(2) site lies on the mirror, and is 2.267 Å from the *Ca*(2)′ site to which it is related by

Tab. 1 Miscellaneous information for metahewettite

a (Å)	12.208(5)	crystal size (μm^3)	2 × 8 × 460
b	3.6011(15)	Radiation	MoK_α
c	18.358(7)	No. of reflections	12219
β (°)	118.538(8)	No. in Ewald sphere	4091
V (Å^3)	709.0(8)	No. unique reflections	1182
Sp. Gr.	*A*2/*m*	No. with ($F_o > 4\sigma F$)	1047
Z	2	R_{merge} %	2.4
		R_1 %	2.4
		wR_2 %	6.7

Cell content: 2 [$Ca(V^{5+}_6O_{16})(H_2O)_3$]
$R_1 = \Sigma(|F_o| - |F_c|) / \Sigma|F_o|$
$wR_2 = [\Sigma w (F_o^2 - F_c^2)^2 / \Sigma w (F_o^2)^2]^{½}$,
$w = 1 / [\sigma^2(F_o^2) + (0.0242\ P)^2 + 2.44\ P]$
where $P = (Max(F_o^2,0) + 2F_c^2) / 3$

Tab. 2. Atom positions and displacement parameters (Å^2) for metahewettite

Site	Occ.	x/a	y/b	z/c	U_{eq}	U_{11}	U_{22}	U_{33}	U_{23}	U_{13}	U_{12}
Ca(1)	0.25	0.5139(15)	0	0.0073(13)	0.0187(19)	0.024(7)	0.0191(11)	0.010(6)	0	0.006(4)	0
Ca(2)	0.25	0.1056(3)	½	0.03623(19)	0.0283(4)	0.0358(16)	0.0235(16)	0.0225(15)	0	0.0115(12)	0
V(1)		0.02216(5)	½	0.19006(3)	0.01103(13)	0.0137(2)	0.0052(2)	0.0170(3)	0	0.0096(2)	0
V(2)		0.39980(5)	0	0.16948(6)	0.01001(13)	0.0126(2)	0.0037(2)	0.0145(3)	0	0.00710(19)	0
V(3)		0.31311(5)	½	0.27707(3)	0.1379(14)	0.0158(3)	0.0094(3)	0.0208(3)	0	0.0124(2)	0
O(1)		–0.0934(2)	½	0.09774(16)	0.0224(5)	0.0205(11)	0.0226(14)	0.0222(12)	0	0.0085(10)	0
O(2)		0.2712(2)	0	0.08403(16)	0.0218(5)	0.0167(11)	0.0238(14)	0.0222(12)	0	0.0071(9)	0
O(3)		0.2582(2)	½	0.34076(16)	0.0216(5)	0.0235(12)	0.0229(13)	0.0243(13)	0	0.0163(10)	0
O(4)		0.1530(2)	½	0.17620(14)	0.0141(4)	0.0152(10)	0.0096(11)	0.0189(11)	0	0.0092(9)	0
O(5)		0.5113(2)	0	0.13539(14)	0.0140(4)	0.0142(9)	0.0113(11)	0.0174(11)	0	0.0083(8)	0
O(6)		0.32830(19)	0	0.25564(14)	0.0131(4)	0.0145(10)	0.0058(10)	0.0211(12)	0	0.0103(9)	0
O(7)		0.0353(2)	0	0.22528(15)	0.0150(4)	0.0241(11)	0.0045(10)	0.0245(12)	0	0.0181(10)	0
O(8)		0.4160(2)	½	0.20396(14)	0.0128(4)	0.0173(10)	0.0037(9)	0.0206(11)	0	0.0116(9)	0
OW(1)		0.6319(3)	½	0.01589(19)	0.0365(7)	0.0385(16)	0.0379(16)	0.0317(16)	0	0.0158(13)	0
OW(2)	0.25	0.0110(10)	0.044(3)	0.0089(7)	0.032(2)						

the 2–fold axis; this close approach does not allow local occupancy of adjacent *Ca*(2) and *Ca*(2)′ sites. The refined site occupancy for the *Ca*(2) site is 0.25; thus half of the locally associated *Ca*(2)–*Ca*(2)′ pairs are occupied by Ca and □ (or □ and Ca) and half by □ and □. Thus both *Ca* sites gave refined site-occupancies of 0.25 within the reported standard deviations, and the two site-occupancies were fixed at this value in the final stages of refinement.

We also analyzed a metahewettite crystal by electron-microprobe analysis (EDS), and found Na to be below detection limit (~0.1 wt.% Na_2O), negating the possibility of a potentially more complex site-occupancy involving Na + Ca + vacancy. On a per-formula-unit (pfu) basis, the two *Ca* sites each provide 0.5 Ca pfu to give a total of 1 Ca pfu. The H_2O group at the OW(2) site was allowed to refine off its initial 2*a* position (0, 0, 0 with site symmetry *2*/*m*), and refined off both the 2-fold axis and the mirror plane at the adjacent 8*j* position (0.0110, 0.044, 0.0089). This results in four equivalent OW(2) sites 0.31–0.44 Å from each other around (0, 0, 0). The refined occupancy for the OW(2) site is 0.25; thus, one of these four OW(2) sites is locally occupied. The fully occupied OW(1) position contributes 2 H_2O groups pfu, and the ¼ occupied OW(2) site contributes 1 H_2O group pfu, to give a total of 3 H_2O groups pfu. The unit-cell dimensions were obtained by least-squares refinement of the positions of 4069 reflections with $I > 10\sigma I$ and are given in Tab. 1, together with other information pertaining to data collection and structure refinement. The structure was refined to a final R_1 index of 2.4 % for 1047 observed ($|F_o| > 4\sigma F$) reflections and 3.0 % for all 1182 data. Refined atom coordinates and anisotropic-displacement parameters are listed in Tab. 2, selected interatomic distances in Tab. 3, and bond valences in Tab. 4.

Tab. 3. Selected interatomic distances (Å) in metahewettite

V(1)–O(1)	1.606(3)		*V*(2)–O(2)	1.604(3)		*V*(3)–O(3)	1.602(3)	
V(1)–O(3)	2.888(3)		*V*(2)–O(5)	1.749(2)		*V*(3)–O(4)	1.947(2)	
V(1)–O(4)	1.733(2)		*V*(2)–O(6)	2.141(2)		*V*(3)–O(5)	1.971(2)	
V(1)–O(7)	1.894(1)	×2	*V*(2)–O(8)	1.887(1)	×2	*V*(3)–O(6)	1.871(1)	×2
V(1)–O(7)	1.987(2)		*V*(2)–O(8)	2.337(2)		*V*(3)–O(8)	2.234(2)	
[5]<*V*(1)–O>	1.823		<*V*(2)–O>	1.934		<*V*(3)–O>	1.916	
Ca(1)–O(3)	2.847(13)		*Ca*(2)–O(1)	2.392(4)		*Ca*(1)–*Ca*(1)′	0.32(3)	
Ca(1)–O(3)	3.158(13)		*Ca*(2)–O(1)	3.130(4)		*Ca*(2)–*Ca*(2)′	2.267(7)	
Ca(1)–O(5)	2.37(3)		*Ca*(2)–O(2)	2.530(3)	×2			
Ca(1)–O(5)	2.49(3)		*Ca*(2)–O(4)	2.349(4)		OW(2)A–OW(2)B	0.31(2)	
Ca(1)–OW(1)	2.264(14)	×2	*Ca*(2)–OW(2)A	2.327(12)	×2	OW(2)A–OW(2)C	0.31(2)	
Ca(1)–OW(1)	2.422(14)	×2	*Ca*(2)–OW(2)B	2.205(10)	×2	OW(2)A–OW(2)D	0.44(2)	
			Ca(2)–OW(2)C	*2.070(10)*	×2			
			Ca(2)–OW(2)D	*1.932(12)*	×2			

4. Description of the structure

4.1. ($V^{5+}O_6$) polyhedra

There are three *V* sites, each of which is fully occupied by V. The *V*(2) and *V*(3) sites are octahedrally coordinated by anions and show variations in individual bond-lengths characteristic for $^{[6]}V^{5+}$. Schindler et al. (2000a, b) have examined the variation in V–O bond-lengths for V^{4+} and V^{5+} in both [5]- and [6]-coordination, and showed that the vanadyl, equatorial and *trans* bonds have typical ranges: 1.54 ≤ vanadyl ≤ 1.78, 1.78 ≤ equatorial ≤ 2.12, 2.12 ≤ *trans* ≤ 2.60 Å, and characteristic stereochemistries (*trans* bonds are *trans* to the vanadyl bonds). Octahedrally coordinated V^{5+} shows two characteristic patterns of [vanadyl + equatorial + *trans*] bonds: [1 + 4 + 1] and [2 + 2 + 2]. Inspection of Tab. 3 shows that the *V*(2) octahedron has a [2 + 2 + 2] configuration: [1.60, 1.75 + 1.89 × 2 + 2.14, 2.34], and the *V*(3) octahedron has a [1 + 4 + 1] configuration: [1.60 + 1.87 × 2, 1.95, 1.97 + 2.23]. All bond-lengths fall in the characteristic ranges for $^{[6]}V^{5+}$. The *V*(1) site is somewhat different. The arrangement of anions around the central cation is octahedral (Fig. 4a) and strongly resembles the arrangements around *V*(2) and *V*(3) (Fig. 4b–c). However, the V(1)–O(3) distance of 2.888 Å (Tab. 3) is much longer than the range for *trans* bonds defined by Schindler et al. (2000a): 2.12–2.60 Å, and the associated bond-valence of 0.05 *vu* (valence units, Tab. 4) is too weak to be normally considered as a bond. Its inclusion or omission in the incident bond-valence sums of the structure is not significant: the sum around *V*(1) is in accord with the valence-sum rule, and the sum around the O(3) anion is low (omitting any possible contribution from hydrogen bonds). Thus the *V*(1)–O(3) bond-length and associated bond-valence suggest that *V*(1) is [5]-coordinated: a square pyramid. The pattern of bond-lengths is as follows: [1.61, 1.73 + 1.89 × 2, 1.99] which is conformable with the [2 + 3] arrangement typical of many [5]-coordinated V^{5+} (Schindler et al. 2000a).

Tab. 4. Bond-valence (*vu*) table for metahewettite

	V(1)	*V*(2)	*V*(3)	Σ	*Ca*(1)	*Ca*(2)	Σ*
O(1)	1.68			1.68		0.32 0.04	2.04
O(2)		1.69		1.69		0.22 ×2↓	1.91
O(3)	0.05		1.70	1.75	0.09 ×½→		1.82
O(4)	1.20		0.67	1.87	0.04 ×½→	0.36	2.23
O(5)		1.14	0.63	1.77			2.06
O(6)		0.40	0.82 ×2↓→	2.04	0.34 ×½→		2.04
O(7)	0.77 ×2↓→ 0.60			2.14	0.24 ×½→		2.14
O(8)		0.79 ×2↓→ 0.23	0.31	2.12			2.12
OW(1)				0	0.45 ×½→ ×2↓ 0.29 ×½→ ×2↓		0.37
OW(2)				0		(0.38 / 0.53) ×½→ ×2↓	0.45
Σ	5.07	5.04	4.95		2.19	1.92 / 2.22	

* summation includes a single Ca contribution
V–O: Tytko et al. (1999); Ca–O: Brese and O'Keeffe (1991)

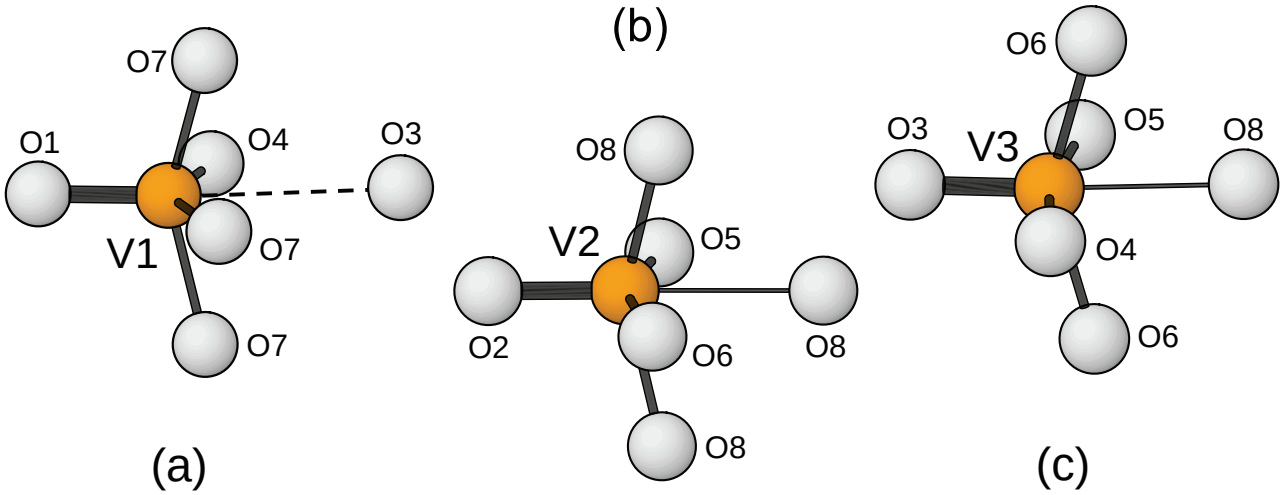

Fig. 4 The three ($V^{5+}O_6$) coordinations in metahewettite. Thick line: strong vanadyl bond, thin line: weak *trans* bond, medium-weight line: equatorial bond, orange circle: V^{5+} cation, grey circle: O^{2-} anion.

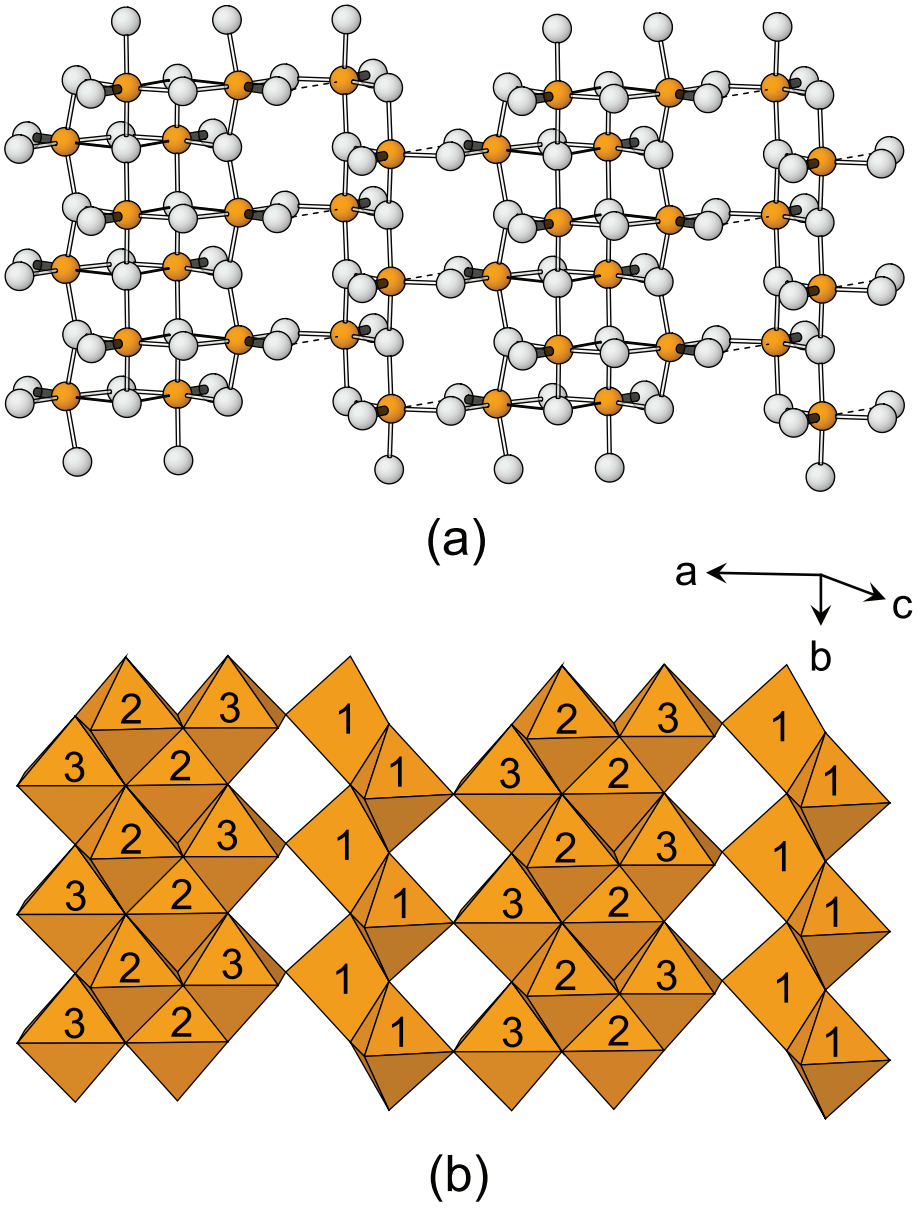

Fig. 5 The $(V^{5+}_6O_{16})^{2-}$ sheet in metahewettite: ball-and-stick representation (**a**) and polyhedron representation (**b**). Legend as in Fig. 4; $(V^{5+}O_6)$ polyhedra: orange shaded. Perspective view of the (001) plane slightly rotated from the plane of the page.

4.2. Anions

The bond-valence table (Tab. 4) confirms that all V is pentavalent. The sites O(1) to O(8) have incident bond-valence sums in the range 1.77–2.33 *vu*, in accord with all of these sites being occupied by O^{2-}. Two sites, labelled OW(1) and OW(2), have incident bond-valence sums of ~0.40 *vu*, and must be (H_2O) groups. The resulting formula: $Ca(V^{5+}_6O_{16})(H_2O)_3$, is neutral and is in accord with the nominal formula of metahewettite.

4.3. Polyhedron linkage

The *V*(1) square pyramids share edges and vertices to form chains extending parallel to **b** with a repeat distance of 3.6 Å. The *V*(2) and *V*(3) octahedra share edges and vertices to form ribbons also extending parallel to **b** (Fig. 5a–b). The chains and ribbons link by sharing polyhedron corners (Fig. 5b) to form sheets of V polyhedra parallel to (001) (Fig. 6). These sheets are linked by interlayer Ca and (H_2O) groups (Fig. 6).

4.4. Interlayer Ca and H_2O

The *Ca*(1) atom is octahedrally coordinated by four (H_2O) groups at the OW(1) site and two O(5) anions, and there are two additional long contacts to the O(3) anion (Fig. 7a). The bond valence requirements of the Ca atom at the *Ca*(1) site are met without the inclusion of the two long *Ca*(1)–O(3) contacts. The Ca atom at the *Ca*(2) site

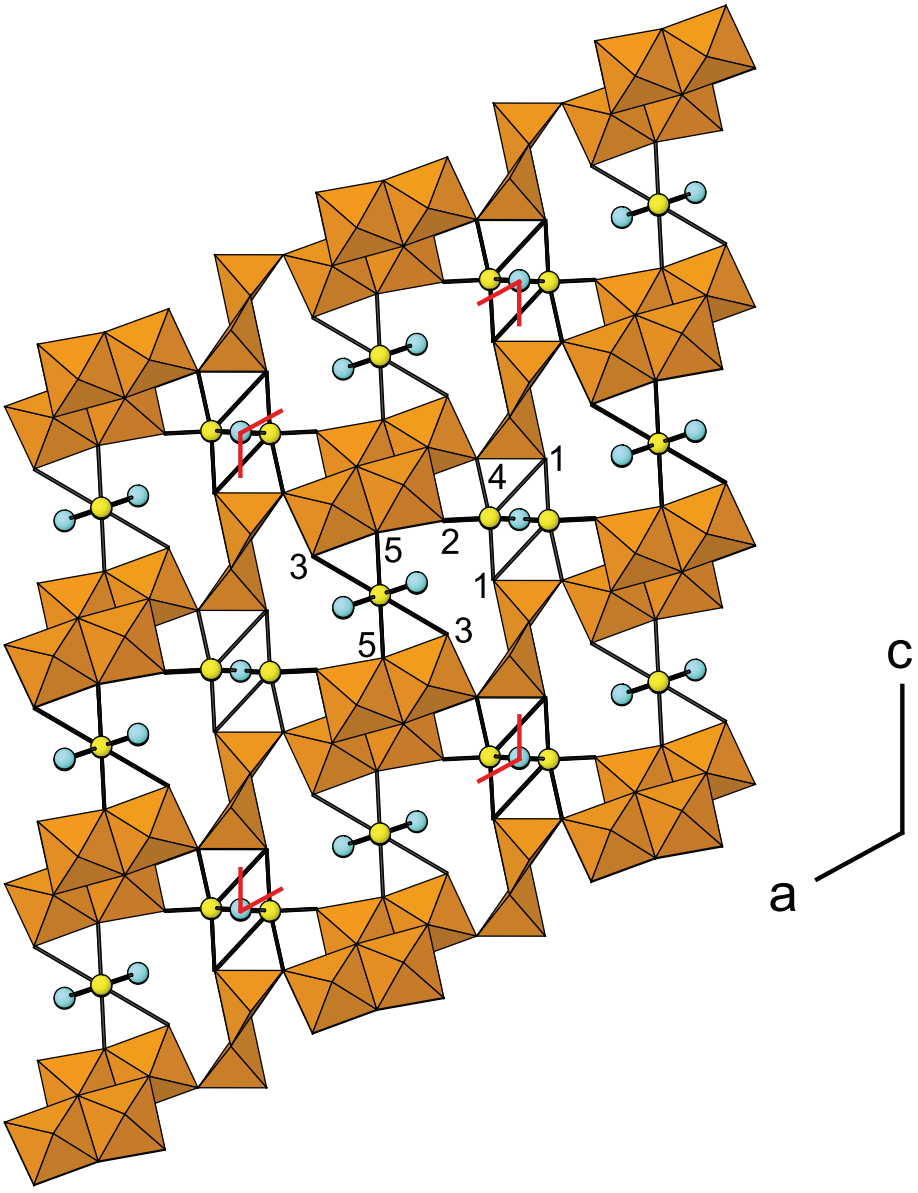

Fig. 6 The $(V^{5+}_{6}O_{16})^{2-}$ sheets and interlayer Ca–H_2O groups in metahewettite, projected down [010]. Unit-cell corners are marked in red. Ca atoms: yellow circles, H_2O groups: blue circles. The mean OW(2) and mean *Ca*(1) sites are displayed; of the paired *Ca*(2) sites shown on both sides of OW(2), only one Ca(2) atom is present locally; central numbers are anion labels.

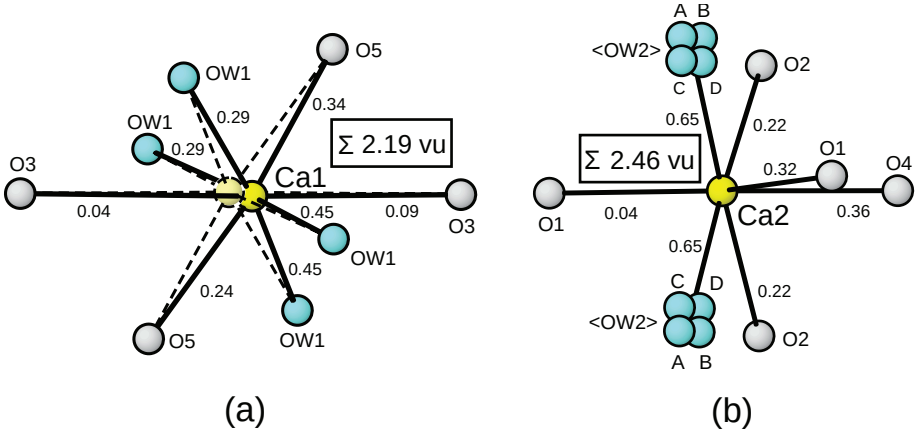

Fig. 7 The coordination of Ca(1) (**a**) and Ca(2) (**b**) in metahewettite. Legend as in Figs 4 and 5, dashed circle/dashed line: associated site vacancy, OW(2) positionally disordered local A, B, C, D site about the central 2*a* (*0, 0, 0*) position. The numbers indicate bond valences in *vu*.

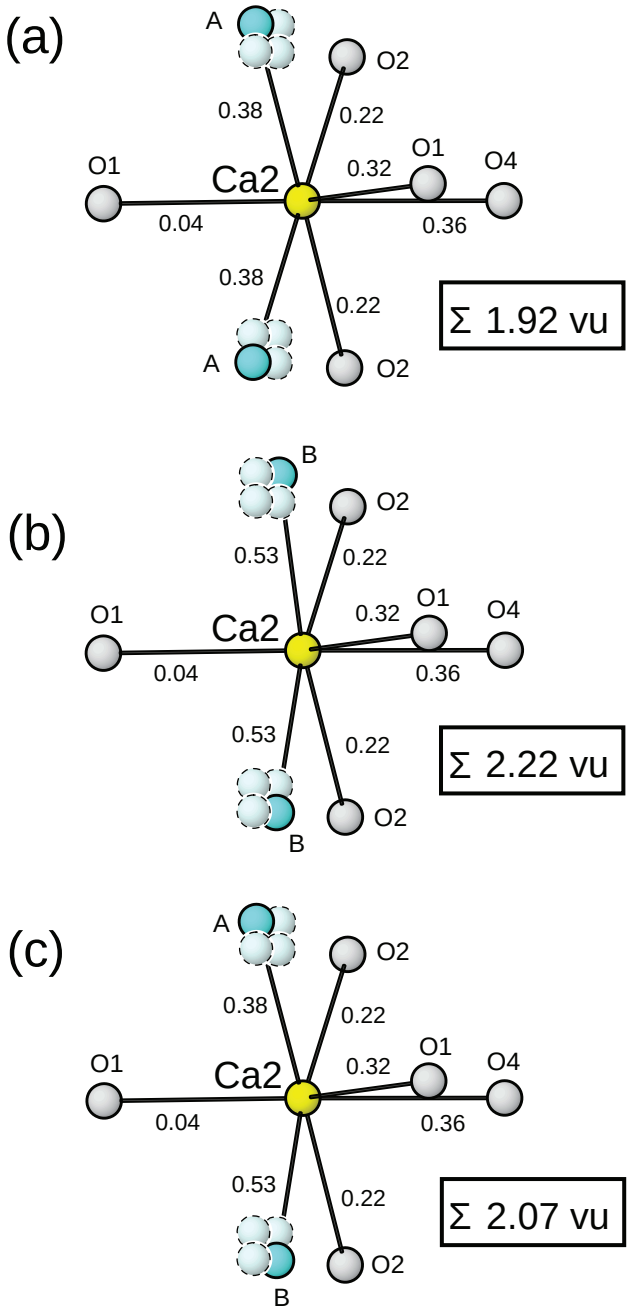

Fig. 8 Possible local OW(2) arrangements about the *Ca*(2) site in metahewettite. Legend as in Fig. 4.

is coordinated by two O(2) anions, an O(1) anion, and an O(4) anion from 2.392 to 2.530 Å, a distant O(1) anion at 3.130 Å and two OW(2) anions (Fig. 7b). The separation between *Ca*(2) and OW(2) in Fig. 8a is shown with a solid line directed toward the centre (at *0,0,0*) of the cluster of four disordered OW(2) sites, and has a calculated bond-valence of 0.65 *vu*. Incorporating the value of 0.65 *vu* into the incident bond-valence at *Ca*(2) results in a sum of 2.46 *vu*, too high for occupancy of *Ca*(2) by Ca. Of the four disordered OW(2) sites (A, B, C, D), three plausible schemes of local order are shown in Fig. 8. If (1) the two OW(2)A sites, or (2) the two OW(2) B sites, or (3) one OW(2)A and one OW(2)B sites, are locally occupied, the incident bond-valence sum at the *Ca*(2) site is in reasonable accord with the valence-sum rule for complete occupancy of *Ca*(2) by Ca (Fig. 8a–c). The OW(2)C–*Ca*(2) and OW(2)D–*Ca*(2) pairs, with associated bond valences of 0.76 and 1.10 vu, respectively, lead to strong violation of the valence-sum rule at the *Ca*(2) site if it is occupied by Ca, and also at the OW(2) site if occupied by an H_2O group. We therefore conclude that where the *Ca*(2) site is locally occupied by Ca, both OW(2)C and OW(2)D sites are locally vacant.

4.5. Local order in the interlayer

The considerable vacancy at the *Ca* sites and positional disorder at both the *Ca* and OW sites greatly complicate the development of a feasible local ordering pattern of Ca and H_2O through the interlayer region. When evaluating hydrogen-bond acceptors around each H_2O group, there is the additional complexity that more than one feasible hydrogen-bond geometry is usually possible, and no electron density corresponding to possible H positions could be reliably identified in the difference-Fourier map. This general character of the interlayer in metahewettite gives some insight as to why the vanadium-bronzes in general are plagued with streaky and problematic X-ray diffraction patterns. Examination of the bond-valence sums at the O atoms shows that the bond-valence requirements of the O(1)–O(5) anions are not satisfied from the V^{5+} contributions alone (Tab. 4), and these anions must receive additional bond-valence from either a nearby Ca atom, or one or more hydrogen bonds from the interlayer region. The bond-valence table was completed by considering only Ca-anion interactions (and does not show how the bond-valence requirements of the O(1)–O(5) anions are satisfied via hydrogen-bonding coupled to local Ca vacancy). The O(1)–O(5) anions are labelled in the central region of Fig. 6; the O(6), O(7) and O(8) anions lie along the 'central spine' of the V(2)–V(3)–V(1) trimer in Fig. 6 and do not bond to the interlayer species. Note that for a locally associated Ca(2)–Ca(2) pair shown in Fig. 6, only one of the two *Ca*(2) sites will be locally occupied, and that for simplicity, only averaged *Ca*(1) and OW(2) sites are shown. The interlayer components Ca(1)–OW(1) and Ca(2)–OW(2) alternate along [100] in Fig. 6 and extend as columns along [010] in Fig. 9. In this figure, we have depicted an arbitrary alternating pattern of Ca occupancy of the *Ca*(1) and *Ca*(2) sites that is consistent with the refined *Ca* site-occupancies, and the OW(2) clusters show all four OW(2) symmetry-related sites disordered about (*0, 0, 0*), with no attempt to indicate a ordered pattern of local occupancy.

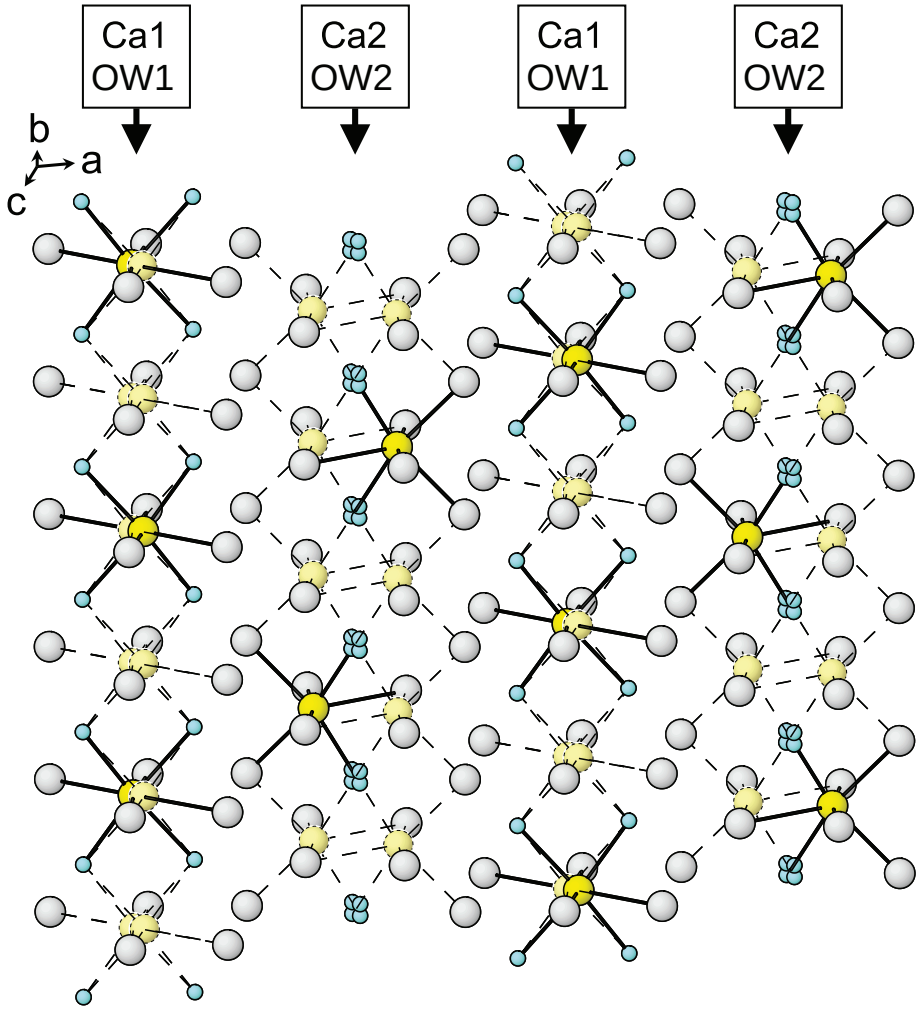

Fig. 9 Arbitrary local scheme of Ca order within a given (001) interlayer region in metahewettite; perspective view with the (001) plane slightly rotated from the plane of the page. Legend as in Figs 4 and 5.

Acknowledgements. We thank Tony Kampf and Michael Schindler for their comments on this paper, V. N. Bobylev, V. S. Gurskii, V. V. Smirnov, G. K. Bekenova and T. V. Dikaya for assistance in the field, and N. A. Pekova for macrophotography. This work was supported by a Canada Research Chair in Crystallography and Mineralogy and by Discovery, Equipment and Major Installation grants of the Natural Sciences and Engineering Research Council of Canada, and by Innovation grants from the Canada Foundation for Innovation to FCH.

Electronic supplementary material. Supplementary crystallographic data for this paper are available online at the Journal web site (http://dx.doi.org/10.3190/jgeosci.167).

References

Agakhanov AA, Karpenko VY, Pautov LA, Uvarova YA, Sokolova E, Hawthorne FC, Bekenova GK (2005) Kyrgyzstanite, $ZnAl_4(SO_4)(OH)_{12}(H_2O)_3$ – a new mineral from the Kara–Tangi, Kyrgyzstan. New Data Mineral 40: 23–28

Ankinovich EA, Podlepaeva NI (1986) A Ca-variety of barnesite from rocks of carbonaceous siliceous vanadium-bearing formation of southern Kazakhstan. Zap Vsesojuz Mineral Obshch 115: 345–351 (in Russian)

Bachmann HG, Barnes WH (1962) The crystal structure of a sodium–calcium variety of metahewettite. Canad Mineral 7: 219–235

Barnes WH (1955) "Hewettite" and "metahewettite". Amer Miner 40: 689–691

Bayliss P (1982) X-ray powder data for hewettite. Mineral Mag 46: 503–504

Bayliss P, Warne SSJ (1979) X-ray powder data for metahewettite. Mineral Mag 43: 550

Brese NE, O'Keeffe M (1991) Bond-valence parameters for solids. Acta Cryst B47: 192–197

Evans HT Jr (1989) The crystal structure of hewettite. Canad Mineral 27: 181–188

Evans HT Jr, Hughes JM (1990) Crystal chemistry of the natural vanadium bronzes. Amer Miner 75: 508–521

Fersman AE (1928) On the morphology and geochemistry of Tyuya–Muyun. In: Proceedings of Exploration for Radium and Radioactive Ores, Vol III. USSR Academy of Sciences Publishing House, Leningrad, pp 1–92 (in Russian)

Hawthorne FC, Cooper MA (2013) The crystal structure of chalcoalumite: mechanisms of Jahn-Teller-driven distortions in $^{[6]}Cu^{2+}$-containing oxysalts. Mineral Mag 77: 2901–2912

Hillebrand WF, Merwin HE, Wright FE (1914) Hewettite, metahewettite, and pascoite, hydrous calcium vanadates. Proc Am Phil Soc 53: 31–54

Lindberg ML, Weeks AD, Thompson ME, Elston DP, Meyrowitz R (1962) Hendersonite, a new calcium vanadyl vanadate from Colorado and New Mexico. Amer Miner 41: 1252–1272

Karpenko VY (2010) Vanadium Mineralization, Connected with Carboniferous Siliceous Schists of South Fergana. Ph.D. thesis, Moscow University Publishing House, Moscow State University, pp 1–24 (in Russian)

Karpenko VY, Pautov LA, Sokolova E, Hawthorne FC, Agakhanov AA, Dikaya TV, Bekenova GK (2004a) Ankinovichite, nickel analogue of alvanite, a new mineral from Kurunsak (Kazakhstan) and Kara–Chagyr (Kirgizia). Zap Vsesojuz Mineral Obshch 133: 59–70

Karpenko VY, Agakhanov AA, Pautov LA, Dikaya TV, Bekenova GK (2004b) New occurrence of nickelalumite on Kara–Chagyr, South Kirgizia. New Data Mineral 39: 32–39

Karpenko VY, Pautov LA, Agakhanov AA (2009) Discovery of low-aluminium nevadaite from the Kara–Chagyr area, Kyrgyzstan. Geol Ore Dep 51: 794–799

Oka Y, Yao T, Sato S, Yamamoto N (1998) Hydrothermal synthesis and crystal structure of barium hewettite: $BaV_6O_{16}.nH_2O$. J Solid State Chem 140: 219–225

Pertlik F, Dunn PJ (1990) Crystal structure of alvanite, $(Zn,Ni)Al_4(VO_3)_2(OH)_{12}\cdot 2H_2O$, the first example of an unbranched zweier–single chain vanadate in nature. Neu Jb Mineral, Mh 9: 385–392

Qurashi MM (1961) The polymorphism and hydration characteristics of hewettite and metahewettite. Canad Mineral 6: 647–662

Scherbakov DI (1924) Deposits of radioactive ores and minerals of Fergana and the tasks of their further research. Materials for Research of Natural Productive Forces of Russia Vol. 47, pp 1–57 (in Russian)

Schindler M, Hawthorne FC, Baur WH (2000a) Crystal chemical aspects of vanadium: polyhedral geometries, characteristic bond valences, and polymerization of (VO_n) polyhedra. Chem Mater 12: 1248–1259

Schindler M, Hawthorne FC, Baur WH (2000b) A crystal chemical approach to the composition and occurrence of vanadium minerals. Canad Mineral 38: 1443–1456

Sheldrick GM (2008) A short history of SHELX. Acta Cryst A64: 112–122

Tytko KH, Mehmke J, Fischer S (1999) Bonding and charge distribution in isopolyoxometalate ions and relevant oxides – a bond valence approach. Struct Bond 93: 129–321

Uvarova YA, Sokolova E, Hawthorne FC, Karpenko V, Agakhanov AA, Pautov LA (2005) The crystal chemistry of the "nickelalumite"-group minerals. Canad Mineral 43: 1511–1519

Vernadsky VI (1922) On a new nickel mineral – kolovratite. Dokl Russ Acad Sci Ser A 1922: 37 (in Russian)

Wadsley AD (1957) Crystal chemistry of non-stoichiometric pentavalent vanadium oxides: crystal structure of $Li_{1+x}V_3O_8$. Acta Cryst 10: 261–267

Weeks AD, Ross DR, Marvin RF (1963) The occurrence and properties of barnesite. $Na_2V_6O_{16}.3H_2O$, a new hydrated sodium vanadate mineral from Utah. Amer Miner 48: 1187–1195

Weeks AD, Lindberg ML, Truesdell AH, Meyrowitz R (1964) Grantsite, a new hydrated sodium calcium vanadate from New Mexico, Colorado, and Utah. Amer Miner 49: 1511–1526